A description of bubble growth and gas release of helium implanted tungsten

S. Sharafat [a,*], A. Takahashi [b], Q. Hu [a], N.M. Ghoniem [a]

[a] University of California Los Angeles, Mechanical and Aerospace Engineering Department, Los Angeles, CA 90095-1597, USA
[b] Tokyo University of Science, Chiba, Japan

ABSTRACT

Bubble growth and gas release during annealing of helium implanted tungsten is described using a Kinetic Monte Carlo approach. Implantation of tungsten with low energy He ions results in the unusual formation of large numbers of oversized surface pores, which eventually lead to drastic changes of the tungsten surface morphology. Traditional rate-theory models are not suitable to simulate surface pore formation. Results of the KMC simulations illustrate the rapid formation of very large helium bubbles and surface pores. The simulation results agree well with observed results of low energy He implanted tungsten experiments, and thus provide an explanation for the observed surface morphology changes caused by low energy He implantation of tungsten.

Published by Elsevier B.V.

1. Introduction

The High Average Power Laser (HAPL) program is a multi-institutional effort to develop Laser Inertial Fusion Energy [1]. Tungsten has been identified as a primary candidate first wall (FW) armor material for a solid wall HAPL IFE chamber design. The implosion of D-T targets produces a spectrum of neutrons, X-rays, and charged particles, such as hydrogen and helium. The energies of helium ions coming from a single 365 MJ D-T target explosion ranges from tens of keV to several MeV, with about 1×10^{20} He-ions below and about 2×10^{20} He above 200 keV. The implantation range of high energy (>200 keV) helium ions is several μm, while that of low energy (<200 keV) helium ions is less than ~0.5 μm in Tungsten. There is compelling experimental evidence showing drastic surface morphology changes of tungsten following implantation with low-energy helium ions. Therefore, low energy helium implantation in Tungsten has become the subject of significant R&D activities for ITER divertor development [2–5].

In support of the HAPL project, low-energy helium implantation in tungsten was investigated at the IEC facility at UW-Madison [6]. Formation of oversized surface bubbles along with drastic surface morphology changes were observed. Traditionally, modeling of helium bubble evolution during irradiation has been based on chemical rate theory also referred to as Master Equation [7,8]. However, rate theory assumes homogenized field parameters and is therefore not suitable for modeling spatially dependent processes, particularly surface pore formation.

Following the approach of Evans et al. [9], we report on our model using Kinetic Monte Carlo (KMC) techniques to simulate migration and coalescence of equilibrium He-bubbles during implantation. Helium bubble migration is based on bubble surface diffusion mechanisms, which leads to rapid bubble growth by coalescence. The KMC simulations agree very well with recent results observed in low energy helium implantation experiments, and hence provide an explanation for the rapid formation of oversized surface pores. The new code is called McHEROS, which stands for Monte Carlo Simulation of helium Bubble Evolution and Resolution.

2. Experimental observations

A number of investigators have published experimental findings showing surface modification caused by low-energy He-ion implantation in Tungsten. In all cases, the formation of high density oversized surface pores (pinholes) and subsurface He-bubbles was observed [2–5]. These findings are somewhat unusual in that large He-bubbles form even when the incident He-energy is less than the displacement threshold energy of tungsten. Depending on the crystallographic direction, the displacement threshold energy of tungsten has been reported to be between 42 and 44 eV, [10]. Nishijima et al. [5] showed that at 1600 °C, implantation of tungsten with helium ions having energies as low as 10 eV results in the formation of large micron-sized surface pores. Although at 10 eV the implantation depth of He in tungsten is of the order of only a few lattice constants (~10 Å) bubbles were observed several micro-meters below the surface. Similarly, implantation with 19 keV helium at temperatures of ~800 °C resulted in the formation of large blisters with a diameter of 0.5–1.0 μm at fluences of 1.7×10^{22} He/m² [11]. At 800 °C blisters are formed, because the high implantation dose rate results in rapid growth of subsurface He-bubbles. However, at high temperatures (2600 °C) the same

* Corresponding author. Tel.: +1 310 794 5990; fax: +1 310 206 4830.
E-mail address: shahrams@ucla.edu (S. Sharafat).

implantation conditions resulted in the formation of a "coral structured" tungsten surface, with "coral horn" structures protruding several micrometers above the surface.

Helium implantation experiments performed at the UW-Madison IEC facility resulted in similar surface morphology altering processes. Fig. 1 shows examples of tungsten surfaces implanted with 30 keV He at various temperatures and fluencies [6]. At a nominal fluence of $\sim 3 \times 10^{22}$ He/m^2, the average surface pore diameter were 15, 50, and 150 nm at 730 °C, 990 °C, and 1160 °C, respectively. With increasing temperatures, surface pore diameter increases and densities drop sharply, indicating a strong bubble coalescence mechanism.

3. Bubble evolution model

Reaction-rate-theory has been widely used to analyze dynamic radiation effects in materials at elevated temperatures [7,8]. Recently, a computer code called HEROS [12] was developed to model space-dependent helium transport and microstructure during irradiation. The HEROS code includes bubble migration by surface- and volume diffusion as well as Brownian Motion and biased bubble migration. The HEROS code was used to simulate the steady state UW-Madison IEC implantation conditions of 30 keV helium with fluences of 3×10^{22} He/m^2 in tungsten. Based on SRIM-2003 SRIM Monte Carlo computer program calculations an implantation profile with a maximum at $\sim$0.2 μm was used and temperatures were assumed to be uniform in the implantation region. In tungsten, about nine vacancies are produced per 30 keV helium ion. The ample supply of vacancies combined with the large helium implantation rates promote the formation of helium-vacancy cluster formation, bubble nucleation, and bubble equilibration between internal pressure and surface tension ($p = 2\gamma/R$; where γ is the surface tension of tungsten and R is the bubble radius).

During the IEC implantation experiments, helium is continuously added to the material. Multi-species helium-vacancy clusters form and continue to trap helium atoms, which leads to formation of stable He-bubble nuclei. However, nucleation of new bubbles is eventually suppressed because growing bubbles provide very strong sinks for the newly implanted helium ions. Thus, nucleation of new bubbles ceases once maximum densities of stable nuclei have been reached. Bubble evolution is therefore separated into two distinct stages: nucleation and growth. To model the IEC helium bubble evolution, it is thus feasible to use the rate-theory nucleation results as initial conditions for the KMC simulation of bubble migration and coalescence. The HEROS code peak bubble concentrations (Fig. 2) were used as the KMC simulation starting conditions [12]. However, it is noted that these conditions only apply to elevated temperatures ($T > 0.3$ Tm $\sim$750 °C for Tungsten).

4. Computer model (McHEROS code)

Details of the McHEROS-code algorithm and structure are reported elsewhere [13], however here we will outline some of the fundamental aspects of the McHEROS code. The kinetics of bubble migration and coalescence are based on Brownian Motion. Both surface- and volume diffusion of bubbles are included, however at IEC relevant temperatures surface diffusion is the predominant diffusion mechanism [14]:

$$D_{\mathrm{B}} = \frac{3\Omega^{4/3}}{2\pi r^4} D_S \tag{1}$$

where D_{B} is the bubble diffusion coefficient, Ω is the atomic volume, r is the bubble radius and D_S is the surface diffusion coefficient, defined as $D_s = D_o\, exp\,(-E_s/kT)$, where D_o is the pre-exponential and E_S is the surface activation energy. Surface activation energies and associated pre-exponential factors for Tungsten were reported by Ehrlich [15]. Depending on the crystollogarphic plane, surface activation energies range from 19.0 to 42.0 kcal/mol (0.92–1.82 eV). At 1000 K the surface diffusivity of W is $\sim$5.8 $\times$ 10^{-8} cm^2/s.

The coalescence process of two bubbles assumes that once they touch, the volumes of the two bubbles will merge and their pressure will instantaneously be in equilibrium with the surface tension ($p = 2\gamma/R$). The size of the new larger bubble is estimated by this simple equilibrium condition. The time involved in forming the new equilibrium bubble has not been estimated, however given the fast surface diffusivity it will be a relatively fast process.
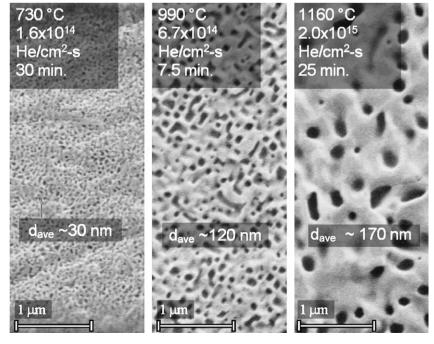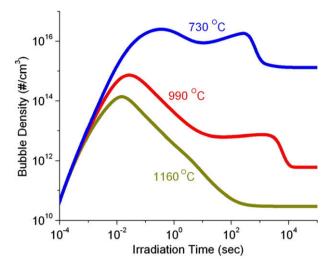

Fig. 1. Micrographs of tungsten surfaces implanted with low energy (30 keV) He at the UW-Madison IEC facility [6].

Fig. 2. Helium bubble density evolution in tungsten as a function of implantation time for IEC conditions (E_{He} = 30 keV, fluence ~3 × 10^{22} He/m^2).

Fig. 3. Snap shots of the time sequence of the McHEROS simulation results of the 30-keV helium implantation at 730 °C (light colored spheres represent matrix or bulk bubbles; darker spheres represent bubbles that have penetrated the surface).

The equilibrium condition however requires that the newly formed bubble instantaneously grows in size to accommodate the internal pressure. However, helium gas pressures indicating solid state conditions have been measured for matrix bubbles in nickel and aluminum [16]. At elevated pressures, plastic deformation of the material surrounding the bubble can occurs, which would result in slowing down or even self-pinning of the bubble. For near surface bubbles, these high pressure conditions generally do not exists because of the abundance of large number of near-surface vacancies. Chernikov et al. [17] measured the mean radius of helium bubbles in Ni as a function of annealing temperature near the surface and in the bulk. Near surface (<1 μm from the surface) bubbles had radii of the order of 70 nm, while the radii of matrix bubbles (>3 μm) were only 2 nm. IEC implantation depths are of the order of 0.2 μm, thus all the bubbles can be assumed to reach equilibrium sizes due to the presence of near surface vacancies.
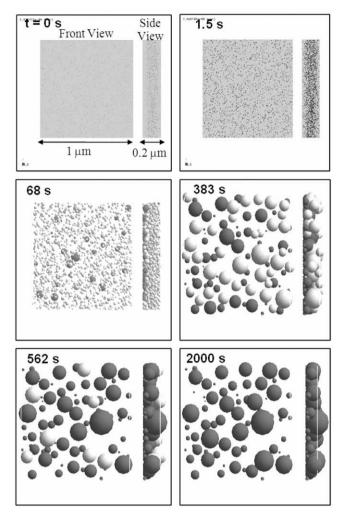
4.1. Initial conditions

As pointed out earlier, the McHEROS code assumes as its initial condition the peak bubble densities at the end of the nucleation phase. The bubbles are distributed with a Gaussian distribution over the implantation range (~0.2 μm in W) for the IEC implanted helium ions (30 keV), see Fig. 3. Furthermore, it is assumed that at the start of the KMC simulation all bubbles have the same average bubble radiuses as calculated by the HEROS code. The initial average bubble radii were determined to be between 0.5 and 1.5 nm, depending on temperature. Table 1 lists the parameters used in the simulation.

5. McHEROS simulation results

Bubble coalescence and growth rates turned out to be extremely rapid. As a result, the bubble densities decreased sharply. To maintain a large enough statistical sampling, a cloning process was adopted as suggested by Evans et al. [9]. It consists of simply doubling the simulation volume as soon as bubble concentrations fall below a threshold value of about 5000 bubbles.

A time sequence of a typical McHEROS simulation results is shown in Fig. 3. The case depicts the 730 °C IEC 30-keV helium implantation experimental conditions. The color scheme is chosen such that as matrix bubbles touch or penetrate the surface, they are colored dark. It is observed that within about 68 s the first sur-

face pores appear and after ~2000 s (at the end of the implantation cycle) almost all of the bubbles have pierced the surface.

Fig. 4 shows the evolution of average diameter of surface pores, and compares the McHEROS simulation results of surface bubble radii with the experimental data. It is seen that the agreement between the McHEROS simulation and the data is astonishingly close, especially for the higher temperature case. The reason is that at lower temperatures (730 °C is slightly below 0.3 Tm), the bubble migration and coalescence is much slower than for higher temperatures. Consequently, our assumption that nucleation of new bubble is absent during the bubble growth stage is no longer strictly valid.

Table 1
Migration and coalescence simulation parameters for IEC low energy He-implantation in W.

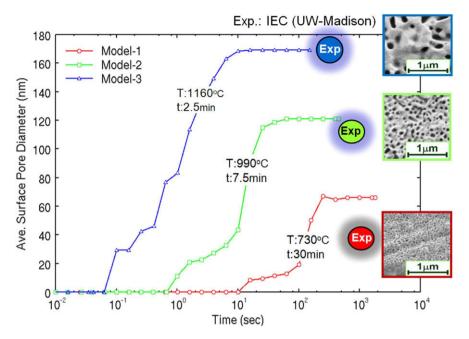| Irradiation temperature (°C)	Initial bubble density (cm^{-3})	Initial bubble radius (nm)	Helium flux (10^{15}/cm^2-s)	Simulation volume (mm^3)
730	10^{17}	0.5	2.2	0.2 × 1.0 × 1
990	10^{15}	1.0	8.8	0.2 × 2.5 × 1
1160	10^{14}	1.5	26.0	0.2 × 5.0 × 1

Fig. 4. Time evolution results of the McHEROS simulation of the average surface bubble diameter as a function of implantation time for 30-keV helium implantation conditions.

6. Conclusions

Implantation of tungsten with low energy He ions results in the unusual formation of large numbers of oversized surface pores, which eventually result in drastic changes of the tungsten surface morphology. Low energy (30 keV) helium implantation experiments between 730 °C and 1160 °C with doses of about ~3 × 10²² m⁻² resulted in the formation of surface pores with average diameters of 170 nm and a density of ~6 × 10¹⁷ m⁻² at 1160 °C.

We developed a KMC-based code to simulate migration and coalescence of near-surface equilibrium helium bubbles (McHEROS Code) using surface diffusion and Brownian Motion based coalescence. Saturated bubble nuclei densities were determined using the HEROS code and used as initial bubble distributions. The abundance of near-surface vacancies and their production during implantation supplies sufficient vacancies for coalescing bubbles to attain equilibrium size and pressure near-surface helium implantation.

Surface pore densities and pore sizes agreed very well with experimental observations. The drastic morphological changes due to low energy helium implantation in tungsten at high temperatures can be explained based on rapid migration and coalescence of equilibrium helium bubbles.

Acknowledgments

References

[1] J.D. Sethian, A.R. Raffray, J. Latkowski, J.P. Blanchard, L. Snead, T.J. Renk, S. Sharafat, J. Nucl. Mater. 347 (3) (2005) 161.
[2] H. Iwakiri, K. Yasunaga, K. Morishita, N. Yoshida, J. Nucl. Mater. 283–287 (2) (2000) 1134.
[3] M. Tokitani, M. Miyamoto, D. Koga, K. Tokunaga, T. Fujiwara, N. Yoshida, S. Masuzaki, N. Ashikawa, T. Morisaki, M. Shoji, A. Komori, J. Nucl. Mater. 337–339 (2005) 937.
[4] N. Yoshida, H. Iwakiri, K. Tokunaga, T. Baba, J. Nucl. Mater. 337–339 (2005) 946.
[5] D. Nishijima, M.Y. Ye, N. Ohno, S. Takamura, J. Nucl. Mater. 329–333 (2004) 1029.
[6] B.B. Cipiti, G.L. Kulcinski, J. Nucl. Mater. 347 (2005) 298.
[7] M. Kiritani, J. Phys. Soc. Jpn. 36 (1973) 95.
[8] N.M. Ghoniem, J.N. Alhajji, J. Nucl. Mater. 136 (1985) 192.
[9] J.H. Evans, R. Escobar Galindo, A. van Veen, Nucl. Instrum. and Meth. B 217 (2004) 276.
[10] A.A. Salomatin, V.A. Mashtakova, B.B. Shishkin, I.P. Chernov, A.P. Mamontov, N.N. Nikitenkov, Atom. Energy. 66 (1) (1989) 53 (Translation).
[11] Tokunaga K. Tokunaga, S. Tamura, N. Yoshida, K. Ezato, M. Taniguchi, K. Sato, S. Suzuki, M. Akiba, J. Nucl. Mater. 329–333 (2004) 757.
[12] Qiyang Hu, Shahram Sharafat, Nasr M. Ghoniem, Fus. Sci. Technol. 52 (3) (2007) 574.
[13] A. Takahashi, S. Sharafat, J. Computational, submitted for publication.
[14] F.A. Nichols, J. Nucl. Mater. 30 (1969) 143.
[15] G. Ehrlich, Surf. Sci. 246 (1991) 1.
[16] W. Jager, R. Manzke, H. Trinkaus, G. Crecelius, R. Zeller, J. Fink, H.L. Bay, J. Nucl. Mater. 111–112 (1982) 674.
[17] V.N. Chernikov, H. Trinkaus, P. Jung, H. Ullmaier, J. Nucl. Mater. 170 (1990) 31.